Journal of Oral Science, Vol. 56, No. 4, 287-293, 2014

Original

Influence of powder composition and morphology on penetration of gray and white ProRoot mineral trioxide aggregate and calcium hydroxide into dentin tubules

Takashi Komabayashi[1)], Leann Long[2)], Chul Ahn[3)], Robert Spears[4)], Qiang Zhu[5)], and Robert C. Eberhart[6)]

[1)]Department of Endodontics, West Virginia University School of Dentistry, Morgantown, WV, USA
[2)]Department of Biostatistics, West Virginia University School of Public Health, Morgantown, WV, USA
[3)]Department of Clinical Sciences, University of Texas Southwestern Medical Center, Dallas, TX, USA
[4)]Department of Biomedical Sciences, Texas A&M Health Science Center, Baylor College of Dentistry, Dallas, TX, USA
[5)]Division of Endodontology, Department of Oral Health and Diagnostic Sciences, University of Connecticut School of Dental Medicine, Farmington, CT, USA
[6)]Department of Surgery, University of Texas Southwestern Medical Center, Dallas, TX, USA

(Received June 18, 2014; Accepted October 22, 2014)

Abstract: This study examined the influence of powder composition and morphology on the penetration of Gray and White ProRoot mineral trioxide aggregate (GMTA, WMTA) and calcium hydroxide (CH) into open dentin tubules. GMTA, WMTA, and CH particle dimensions were analyzed by flow particle image analysis (FPIA). Penetration of open dentin tubules into dentin discs was studied by scanning electron microscopy. Five samples of each material were randomly selected and prepared for this study. The GMTA averages for length (μm), width (μm), perimeter (μm), and aspect ratio were 1.94 ± 1.65, 1.43 ± 1.19, 5.61 ± 4.27, and 0.76 ± 0.14, respectively. Corresponding averages for WMTA were 2.04 ± 1.87, 1.49 ± 1.33, 5.88 ± 4.81, and 0.76 ± 0.14, and for CH were 2.26 ± 1.99, 1.62 ± 1.46, 6.70 ± 5.60, and 0.74 ± 0.15, respectively. The rank order of the averages for particle length, width and perimeter from the largest to the smallest material was CH > WMTA > GMTA. The rank order of the averaged aspect ratios was GMTA > WMTA > CH. SEM showed that all three materials, when deposited and agitated on dentin discs, penetrated the open dentin tubules. Tubule occlusion occurred as particle surface concentrations increased. Significant differences in particle length, width, perimeter, and aspect ratio were observed for GMTA, WMTA, and CH ($P < 0.0001$ in all cases). All particle types penetrated into open tubules when agitated on dentin discs; all tubules were eventually occluded as particle concentrations grew.
(J Oral Sci 56, 287-293, 2014)

Keywords: calcium hydroxide; dentin tubule; image analysis; mineral trioxide aggregate; morphology.

Correspondence to Dr. Takashi Komabayashi, Department of Endodontics, West Virginia University School of Dentistry, One Medical Center Drive, P.O. Box 9450, Health Science Center North, Morgantown, WV 26506-9450, USA
Fax: +1-304-293-7649
E-mail: takomabayashi@hsc.wvu.edu & ICD38719@nifty.com

doi.org/10.2334/josnusd.56.287
DN/JST.JSTAGE/josnusd/56.287

Introduction

Gray ProRoot mineral trioxide aggregate (GMTA) (Dentsply Tulsa Dental, Johnson City, TN, USA) was patented in 1995 as a root-end filling material (1-3). White ProRoot mineral trioxide aggregate (WMTA) from the same vendor was later introduced (4), with iron compounds extracted and lower aluminoferrite

concentration, to decrease anterior tooth discoloration (5-8). Mineral trioxide aggregate (MTA) has two phases, calcium oxide and calcium phosphate; the calcium oxide reacts with tissue fluid to form calcium hydroxide (CH) (9-12). The chemical and physical characteristics (4,13-20) and biocompatibility (14,17,21-23) of MTA have been reported. MTA and CH have been clinically studied for use in primary molar pulpotomies (24), as pulp capping agents in permanent premolars (25), and as regenerative treatments for immature, traumatized teeth with apical periodontitis (26).

GMTA, WMTA, and CH particles contact pulp and dentin during topical application. The morphologic properties of the particulates are believed to contribute to, if not determine, pulp cellular response. *In vitro* studies suggest that surface microtopography influences primary protein deposition and organization, and the resultant cell adhesion and proliferation, differentiation and local factor production (27-29). The early cellular response is hypothesized to be affected by the morphology of unset MTA particles, as it takes many hours for MTA to set (30,31). In dentin, the reported size of dentin tubules (approximately 2 to 5 μm in diameter) is of the same order as GMTA, WMTA, and CH particle sizes (32-34) and thus might penetrate these pores. Clinical implications of this hypothesis include a possible hydraulic seal mechanism in MTA (32,33) and antimicrobial action of CH inside the dentin tubules (34). Accordingly, a precise comparison of the dimensional characteristics of unset GMTA, WMTA, and CH may be of clinical significance in endodontics.

Our previous studies examined particle morphologies of GMTA, WMTA, and research grade CH (32-34). We speculated that the size and shape of CH particles allows direct penetration into open dentin tubules, but did not directly observe, or assess the potential of, these particles to enter these tubules. The present study provides direct observation of particle behavior in the vicinity of the open dentin tubules, combined with size analysis, to answer this question.

Materials and Methods

Flow particle image analyzer

Image analysis technology is used in many industries to optimize product and process performance (35-37). A flow particle image analyzer (FPIA-3000; Sysmex, Kobe, Japan) analyzes the size and shape of particles in emulsions and suspensions, and produces quantitative shape information expressed as the morphological parameters of particles. This technique provides statistically valid sizes and shapes of large numbers of particles (32-34). In low-power mode, "coarse" particles ranging in size from 6 to 160 μm are observed, while the high-power field (HPF) mode allows the analysis of finer particles, between 1.5 and 40 μm, with a minimum detectable level of 0.5 μm for selected analysis parameters. Previous studies indicated that the HPF mode was suitable for the study of finer-grained MTA, Portland cement and CH (32-34); thus, the HPF mode was used for this study.

Gray ProRoot MTA (GMTA; Lot #10004117, Dentsply Tulsa Dental), White ProRoot MTA (WMTA; Lot #09003851, Dentsply Tulsa Dental), and research grade calcium hydroxide (CH; Lot #31H3445, C-7887, Sigma-Aldrich, St. Louis, MO, USA) particles were selected for analysis. Ten milligrams of MTA and CH were mixed with 10 mL and 15 mL of alcohol, respectively, followed by sonication for 1 min to create a homogeneous particle suspension. Suspensions drawn from these sources were examined by the FPIA-3000 flow particle image analyzer. Polystyrene latex particles (2 μm, Polymer Microspheres 5200A; Duke Scientific Corporation, Fremont, CA, USA) were used as calibration objects to adjust the focus before the MTA and CH samples were evaluated. Five milliliters of this suspension was added to FPIA. The final analyzed volume was set at 0.35 μL.

Five sample groups were randomly prepared. Digital images of the sample particles were automatically collected by the FPIA machine in HPF mode. Particle size was analyzed using computer software (Sysmex) in terms of length, width and perimeter; particle shape was described by the aspect ratio. Definitions of particle length, width, perimeter and aspect ratio are summarized in Table 1.

Statistical analysis

Means, standard deviation, and number of particles were calculated for GMTA, WMTA and CH samples. One-way analyses of variance (ANOVA) were used to identify any significant differences in length, width, perimeter, and aspect ratio among the five sample groups. A P-value less than 0.05 was considered statistically significant. Pairwise comparisons among GMTA, WMTA, and CH were conducted by Student's t-test with Bonferroni's correction to identify significant differences in length, width, perimeter and aspect ratio. Length was classified into five categories, category 1 (0.5-1.0 μm), category 2 (1.0-1.5 μm), category 3 (1.5-2.0 μm), category 4 (2.0-2.5 μm), and category 5 (over 2.5 μm), in order to test for significant differences in the frequency of particles among the five length categories for the various materials. Chi-squared goodness-of-fit test was used to identify differences, if any, from the expected number of particles

Table 1 Definitions of particle length, width, perimeter, and aspect ratio

Parameters	Unit	Explanation
Particle size		
Length	μm	The length of the longer axis when the particle image is bounded by two pairs of parallel lines
Width	μm	The length of the shorter axis when the particle image is bounded by two pairs of parallel lines
Perimeter	μm	Length of the particle perimeter
Particle shape		
Aspect ratio (W/L)	None	The ratio between length and width

Table 2 Results for particle length, width, perimeter, and aspect ratio

Parameters	CH	GMTA	WMTA	*P* value
Particle size				
Length (μm)	2.26 ± 1.99	1.94 ± 1.65	2.04 ± 1.87	<0.001
Width (μm)	1.62 ± 1.46	1.43 ± 1.19	1.49 ± 1.33	<0.001
Perimeter (μm)	6.70 ± 5.60	5.61 ± 4.27	5.88 ± 4.81	<0.001
Particle shape				
Aspect ratio (W/L)	0.74 ± 0.15	0.76 ± 0.14	0.76 ± 0.14	<0.001
The number of particles	46,818	64,268	51,766	

Values are mean with standard deviation.

among the five categories of length. ANOVA was used to test for significant differences in width, perimeter and aspect ratio among the five length categories. All statistical tests were performed using SAS 9.3 (SAS Institute, Cary, NC, USA).

Dentin sample preparation and scanning electron microscope examination

Four fully erupted, defect-free human posterior teeth, approved by the research ethics committee, Texas A&M Health Science Center Baylor College of Dentistry (No. 2011-06), were extracted by local dentists for treatment reasons unrelated to this study. After being cleaned and washed with water, teeth were sectioned perpendicular to the long axis just inside the DEJ with a slow-speed diamond saw (Isomet 1000, Buehler, Ltd., Lake Bluff, IL, USA) at 300 rpm and hand-polished through 400-grit silicon carbide abrasive paper to obtain discs nominally 0.5 mm thick. Smear layers were removed by immersing the discs in 17% EDTA (1 min), followed by in 5% NaOCl (1 min). Sections were washed with distilled water and dried, and then prepared for scanning electron microscope (SEM; JSM-6300, JEOL USA, Peabody, MA, USA) evaluation at 15 kV by sputter coating the surface with a thin gold coating under a vacuum (Desk II; Denton Vacuum LLC, Moorestown, NJ, USA).

SEM was used to evaluate the following representative digital images at low and high magnification: 1) open dentin tubules; and 2) three materials agitated on dentin disc in order to determine whether the particles occluded the open dentin tubules. The three materials were mixed with distilled water to form a paste in accordance to manufacturer's recommendation for GMTA and WMTA and clinically applicable consistency for CH. The materials were then agitated on the dentin discs immediately after mixture of materials to mimic the clinical procedure. The estimated percentage of particle-filled open tubules was calculated from the frequency distributions of open tubules for each material.

Results

Flow particle image analysis

Total numbers of particles analyzed by FPIA were 46,818 (CH), 64,268 (GMTA), and 51,766 (WMTA). The results for particle length, width, perimeter, and aspect ratio are averaged and summarized in Table 2. Significant differences between the three materials were observed for all dimensions and aspect ratios ($P < 0.001$ in each case).

The frequency of open dentin tubule diameters is compared in Table 3 with the particle length frequency distributions for CH, GMTA, and WMTA, tabulated according to the previously described particle length categories, recapitulating the statistically significant differences between them. Open tubule diameters were obtained from measurements of representative dentin SEM images (Figs. 1A, 1B). Figure 2 displays the

Table 3 Comparison of open tubule diameter frequencies with particle length frequencies for CH, GMTA, and WMTA

Length category (μm)	Open tubule diameter	CH	GMTA	WMTA	*P* value
0.5 - 1.0	0.6%	19.2%	25.9%	24.9%	$P < 0.0001$
1.0 - 1.5	4.6%	27.1%	30.2%	29.6%	$P < 0.0001$
1.5 - 2.0	13.2%	17.1%	15.7%	16.0%	$P < 0.0001$
2.0 - 2.5	50.3%	10.7%	9.1%	9.0%	$P < 0.0001$
>2.5	30.9%	25.9%	19.1%	20.5%	$P < 0.0001$

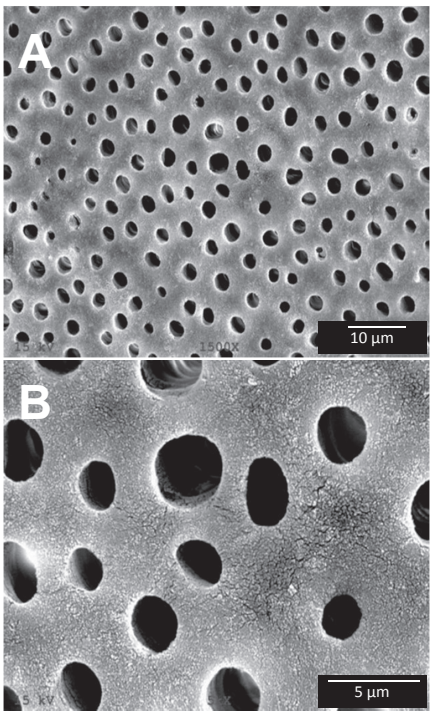

Fig. 1 Open dentin tubules (untreated control tooth group) A; 1,500×, B; 5,000×

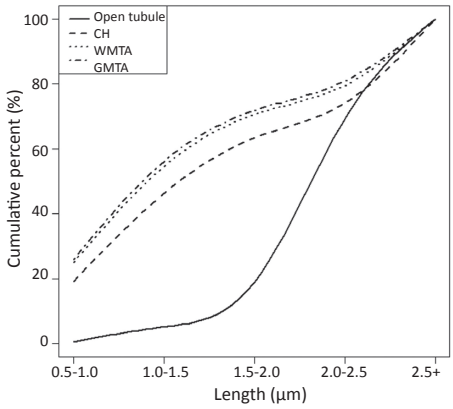

Fig. 2 Distribution of cumulative material particle sizes relative to open tubule diameters

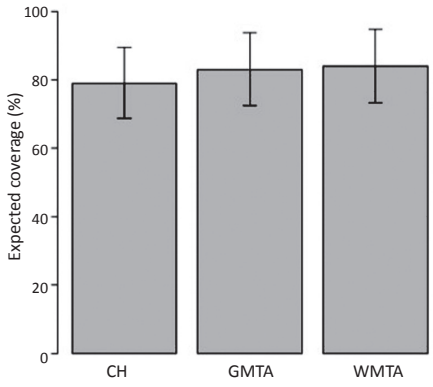

Fig. 3 Expected percentage of open tubules to be filled by particles

cumulative distributions of CH, WMTA, and GMTA particle lengths, and the cumulative open tubule diameter distributions. The expected percentage of open tubules to be filled is calculated using the frequency distributions of CH, GMTA, and WMTA particles, as well as that of open tubules. Figure 3 presents the results in terms of estimated percentages of open tubules covered for each of the three materials and the respective 95% confidence intervals. For the observed distributions in Fig. 3, CH, GMTA, and WMTA are expected to have 79%, 83%, and 84% coverage, respectively.

Particle images by scanning electron microscopy

Figure 4 shows images of coated tubule-containing dentin discs with particles distributed during overlaying by agitation. GMTA and WMTA covered almost all the open dentin tubules, while some open tubules remained on the CH-treated dentin discs. Individual particles can be seen within open tubules in all three material categories. Complete coverage of the tubule, with an apparent "fracturing" of the overlayer is seen frequently.

Discussion

Flow particle image analysis (FPIA) allows measurement

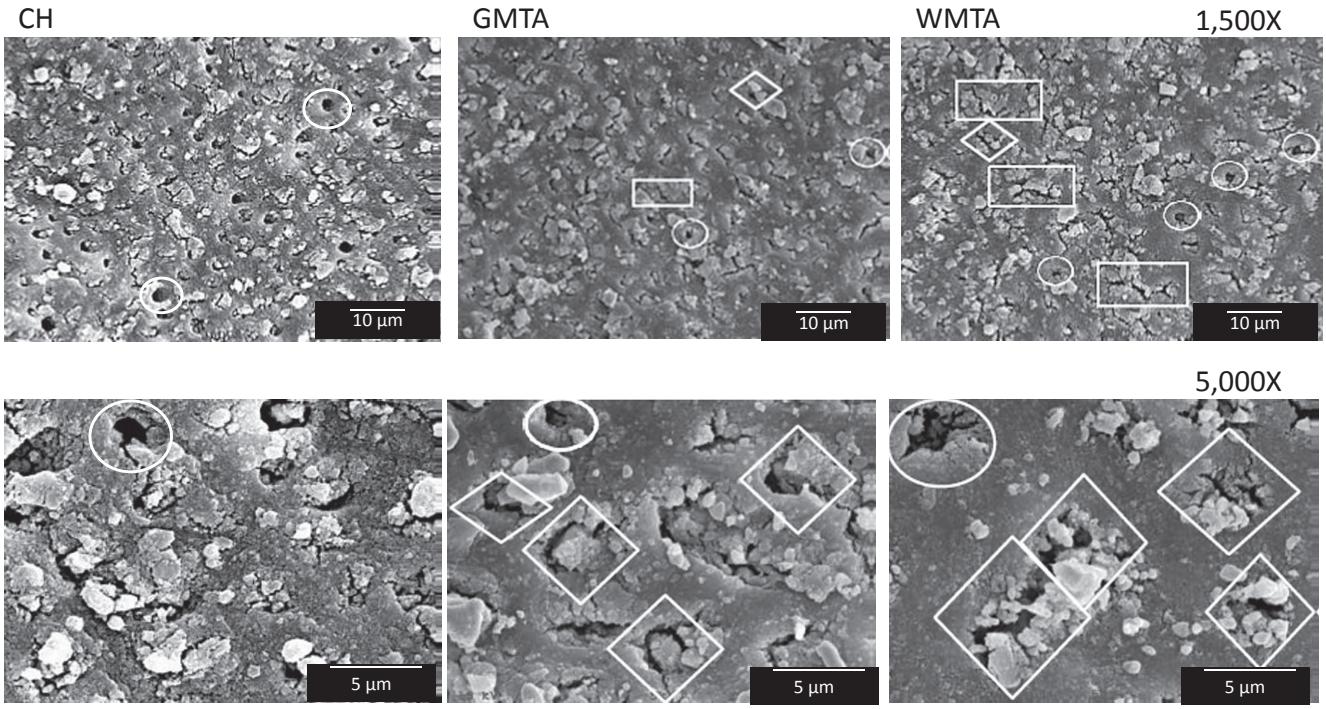

Fig. 4 Three materials were agitated on dentin discs to determine whether powder/paste occludes open dentin tubules (experimental treated teeth group)

- Particles embedded within open dentin tubules or located on the surface over open dentin tubules are denoted by diamonds.
- Particles aggregated with amorphous powder film, but may be covering open dentin tubules denoted by rectangles.
- Unfilled open dentin tubules are denoted by circles.

of large numbers of individual particle sizes and shapes, whereas SEM provides results of agglomerations of particles. Combining FPIA with SEM we can determine the distribution of powder particle sizes and observe the diameter and occlusion of dentin tubules by the three materials.

FPIA machine analysis yielded cumulative percentages of particle lengths between 0.5 and 2.0 µm, which is less than the reported diameters of tubules in root dentin (72%, 71%, and 63% for GMTA, WMTA, and CH, respectively). The approximately 8 to 9% difference in the cumulative percentages of MTA and CH particles at this size suggests that the geometry of small MTA particles makes these particles more likely to enter open dentin tubules, as compared with the CH fine particles. Regarding the difference between GMAT and WMTA, Comin-Chiaramonti et al. reported that White MTA is largely free of any celite component (38). This may possibly explain the small, approximately 1%, difference in the cumulative percentages of the two MTA particle forms. Asgary et al. reported that WMTA possessed smaller particle sizes than GMTA (39); however, our results suggest the opposite.

The results show open dentin tubules ranged in diameter from 0.9 to 3.2 µm and the average size of open dentin tubules was 2.23 µm. Using these data, the overlays of particle histograms with those for open dentin tubules was compared, looking for overlaps and the potential for open dentin tubules to be infiltrated. Because both GMTA and WMTA have higher concentrations of small particles than CH, particularly for lengths of 0.5-1.5 µm, more open tubules can be penetrated by these powders. While the distribution of cumulative material particle sizes relative to open tubule diameters leads us to expect more open tubules to be filled by WMTA and GMTA than by CH. The estimated coverage percentages and their respective 95% confidence intervals revealed no differences in expected coverage of open tubules by these three materials. Because more than 95% of tubule diameters are greater than one micron, more than 50% of all particles are below the 1.5-2.0 µm tubule diameter threshold. Hence, it appears that if appropriately presented, most particles could fit within the dentin tubules, even when particle long axes are parallel to the dentin plane. Clinically, all the dentin tubules could be filled by addition of repeated application of material paste into the root canals.

SEM showed that coverage of open dentin tubules

can be described by several types. Some particles were embedded within open dentin tubules or located on the surface over open dentin tubules. Some particles aggregated with amorphous powder film and covered the dentin tubules. A small portion of dentin tubules was not covered (circles). Overall, it appears that there is some particle entry into the open dentin tubules.

A potential advantage of FPIA is the capacity to determine particle shape and size (32-34). The aspect ratio is one method of determining particle shape. The rank order of the overall average aspect ratio, from the largest to the smallest material particles, was GMTA > WMTA > CH. The aspect ratio was the highest for category 1 particles (0.5-1.0 μm), but was the lowest for category 5 (over 2.5 μm). As particle size increased, particle shapes became less elongated, i.e., broader. According to our estimates, it may be easier for a shorter single particle to pass into dentin tubules, particularly if assisted by an initial inflow of filling liquid. However, as particle density increases, both flow patterns and particle-particle interactions become more complex. It thus becomes difficult to predict tubule filling.

MTA powder is basically a mixture of Portland cement, bismuth oxide, and gypsum. The morphology of the initial particles becomes less apparent when mixed with water. The smooth structure comprised of fine particle agglomerates could be considered a hydration product that may be responsible for causing the particles to adhere to one another. Further research and consideration needs to be given to mixing powder-water ratio, moisture supplementation, and its duration with respect to porosity. In addition, further studies aimed at maintaining the biological qualities of MTA and CH and evaluating the initial cellular response of unset MTA particles with regard to particle size and shape characterization are suggested by our research. These would also be applicable to other emerging areas of endodontic research, such as stem cell/scaffold research, the dentin-material interface, biomineralization, and nanotechnology.

1. The size and shape of the GMTA, WMTA, and CH powders in this study permit direct penetration into open dentin tubules. The cumulative percentages of particle lengths between 0.5 and 2.0 μm, less than the reported diameters of most tubules in root dentin, were 72%, 71%, and 63% for GMTA, WMTA, and CH, respectively.
2. The rank order of the overall average of length, width, and perimeter from the largest to the smallest material was CH > WMTA > GMTA. Category 2 (1.0-1.5 μm) had the highest number in all the GMTA, WMTA, and CH groups.
3. The rank order of the overall average aspect ratio from the largest to the smallest material in the groups was GMTA > WMTA > CH. The aspect ratio was the highest in category 1 (0.5-1.0 μm), and was the lowest in category 5 (over 2.5 μm). As particle size increased, particle shape broadened from the elongated forms of smaller particles.
4. There were significant differences in length, width, perimeter, and aspect ratio among material groups GMTA, WMTA, and CH ($P < 0.0001$ in each case).
5. Using the frequency distributions of CH, GMTA, and WMTA particles, as well as that of open tubules, the expected percentage of open tubules to be covered (filled) by CH, GMTA, and WMTA was 79%, 83%, and 84%, respectively.
6. Presenting trace amounts of the three powdered materials on agitated dentin disc occluded open dentin tubules. GMTA and WMTA covered almost all the open dentin tubules, while more open dentin tubules were seen on the research grade $Ca(OH)_2$-treated disc samples.

Acknowledgments

The authors would like to thank Dr. Kevin Dahl, Mr. Andrew Jones, Mr. Terry Stauffer, Dr. Yoshiyuki Inoue, and Mr. Koji Sanada (Malvern Instrument Inc. [USA/UK] / Hosokawa Micron Corporation [Japan]) for analyzing samples and providing technical information. This study was supported by NIH UL1TR0000451 and U54GM104942. The authors are also grateful to Poorva Gharpure, BDS, for SEM technical support.

References

1. Lee SJ, Monsef M, Torabinejad M (1993) Sealing ability of a mineral trioxide aggregate for repair of lateral root perforations. J Endod 19, 541-544.
2. Torabinejad M, Watson TF, Pitt Ford TR (1993) Sealing ability of a mineral trioxide aggregate when used as a root end filling material. J Endod 19, 591-595.
3. Torabinejad M, White DJ (1995) Tooth filling material and use. US Patent 5,769,638, May 16.
4. Camilleri J, Montesin FE, Brady K, Sweeney R, Curtis RV, Ford TR (2005) The constitution of mineral trioxide aggregate. Dent Mater 21, 297-303.
5. Ferris DM, Baumgartner JC (2004) Perforation repair comparing two types of mineral trioxide aggregate. J Endod 30, 422-424.
6. Moghaddame-Jafari S, Mantellini MG, Botero TM, McDonald NJ, Nör JE (2005) Effect of ProRoot MTA on pulp cell apoptosis and proliferation in vitro. J Endod 31, 387-391.
7. Dammaschke T, Gerth HU, Züchner H, Schäfer E (2005) Chemical and physical surface and bulk material characterization of white ProRoot MTA and two Portland cements. Dent Mater 21, 731-738.

8. Asgary S, Parirokh M, Eghbal MJ, Brink F (2005) Chemical differences between white and gray mineral trioxide aggregate. J Endod 31, 101-103.
9. Torabinejad M, Hong CU, McDonald F, Pitt Ford TR (1995) Physical and chemical properties of a new root-end filling material. J Endod 21, 349-353.
10. Torabinejad M, Hong CU, Pitt Ford TR, Kettering JD (1995) Antibacterial effects of some root end filling materials. J Endod 21, 403-406.
11. Koh ET, McDonald F, Pitt Ford TR, Torabinejad M (1998) Cellular response to mineral trioxide aggregate. J Endod 24, 543-547.
12. Holland R, de Souza V, Nery MJ, Otoboni Filho JA, Bernabé PF, Dezan Júnior E (1999) Reaction of rat connective tissue to implanted dentin tubes filled with mineral trioxide aggregate or calcium hydroxide. J Endod 25, 161-166.
13. Estrela C, Bammann LL, Estrela CR, Silva RS, Pecora JD (2000) Antimicrobial and chemical study of MTA, Portland cement, calcium hydroxide paste, Sealapex and Dycal. Braz Dent J 11, 3-9.
14. Abdullah D, Ford TR, Papaioannou S, Nicholson J, McDonald F (2002) An evaluation of accelerated Portland cement as a restorative material. Biomaterials 23, 4001-4010.
15. Funteas UR, Wallace JA, Fochtman EW (2003) A comparative analysis of mineral trioxide aggregate and Portland cement. Aust Endod J 29, 43-44.
16. Asgary S, Parirokh M, Eghbal MJ, Brink F (2004) A comparative study of white mineral trioxide aggregate and white Portland cements using X-ray microanalysis. Aust Endod J 30, 89-92.
17. Camilleri J, Montesin FE, Di Silvio L, Pitt Ford TR (2005) The chemical constitution and biocompatibility of accelerated Portland cement for endodontic use. Int Endod J 38, 834-842.
18. Song JS, Mante FK, Romanow WJ, Kim S (2006) Chemical analysis of powder and set forms of Portland cement, gray ProRoot MTA, white ProRoot MTA, and gray MTA-Angelus. Oral Surg Oral Med Oral Pathol Oral Radiol Endod 102, 809-815.
19. Islam I, Chng HK, Yap AU (2006) Comparison of the physical and mechanical properties of MTA and Portland cement. J Endod 32, 193-197.
20. Oliveira MG, Xavier CB, Demarco FF, Pinheiro AL, Costa AT, Pozza DH (2007) Comparative chemical study of MTA and Portland cements. Braz Dent J 18, 3-7.
21. Holland R, de Souza V, Murata SS, Nery MJ, Bernabé PF, Otoboni Filho JA et al. (2001) Healing process of dog dental pulp after pulpotomy and pulp covering with mineral trioxide aggregate or Portland cement. Braz Dent J 12, 109-113.
22. Saidon J, He J, Zhu Q, Safavi K, Spångberg LS (2003) Cell and tissue reactions to mineral trioxide aggregate and Portland cement. Oral Surg Oral Med Oral Pathol Oral Radiol Endod 95, 483-489.
23. Min KS, Kim HI, Park HJ, Pi SH, Hong CU, Kim EC (2007) Human pulp cells response to Portland cement in vitro. J Endod 33, 163-166.
24. Sonmez D, Sari S, Cetinbaş T (2008) A Comparison of four pulpotomy techniques in primary molars: a long-term follow-up. J Endod 34, 950-955.
25. Accorinte Mde L, Holland R, Reis A, Bortoluzzi MC, Murata SS, Dezan E Jr et al. (2008) Evaluation of mineral trioxide aggregate and calcium hydroxide cement as pulp-capping agents in human teeth. J Endod 34, 1-6.
26. Cotti E, Mereu M, Lusso D (2008) Regenerative treatment of an immature, traumatized tooth with apical periodontitis: report of a case. J Endod 34, 611-616.
27. Martin JY, Schwartz Z, Hummert TW, Schraub DM, Simpson J, Lankford J Jr et al. (1995) Effect of titanium surface roughness on proliferation, differentiation, and protein synthesis of human osteoblast-like cells (MG63). J Biomed Mater Res 29, 389-401.
28. Massaro C, Baker MA, Cosentino F, Ramires PA, Klose S, Milella E (2001) Surface and biological evaluation of hydroxyapatite-based coatings on titanium deposited by different techniques. J Biomed Mater Res 58, 651-657.
29. Zhao G, Zinger O, Schwartz Z, Wieland M, Landolt D, Boyan BD (2006) Osteoblast-like cells are sensitive to submicron-scale surface structure. Clin Oral Implants Res 17, 258-264.
30. Torabinejad M, Chivian N (1999) Clinical applications of mineral trioxide aggregate. J Endod 25, 197-205.
31. Kogan P, He J, Glickman GN, Watanabe I (2006) The effects of various additives on setting properties of MTA. J Endod 32, 569-572.
32. Komabayashi T, Spångberg LS (2008) Comparative analysis of the particle size and shape of commercially available mineral trioxide aggregates and Portland cement: a study with a flow particle image analyzer. J Endod 34, 94-98.
33. Komabayashi T, Spångberg LS (2008) Particle size and shape analysis of MTA finer fractions using Portland cement. J Endod 34, 709-711.
34. Komabayashi T, D'souza RN, Dechow PC, Safavi KE, Spångberg LS (2009) Particle size and shape of calcium hydroxide. J Endod 35, 284-287.
35. Sieracki CK, Sieracki ME, Yentsch CS (1998) An imaging-in-flow system for automated analysis of marine microplankton. Mar Ecol Prog Ser 168, 285-296.
36. Abriak NE, Gandola F (1999) Image analysis techniques applied to the study of granular materials in silo. Powder Handling Proc 11, 49.
37. Svoboda V, Doering H, Garche J (2005) The influence of fast charging on the performance of VRLA batteries. J Power Sources 144, 244-254.
38. Comin-Chiaramonti L, Cavalleri G, Sbaizero O, Comin-Chiaramonti P (2009) Crystallochemical comparison between Portland cements and mineral trioxide aggregate (MTA). J Appl Biomater Biomech 7, 171-178.
39. Asgary S, Parirokh M, Eghbal MJ, Stowe S, Brink F (2006) A qualitative X-ray analysis of white and grey mineral trioxide aggregate using compositional imaging. J Mater Sci Mater Med 17, 187-191.